FERRARIS, G. & CATTI, M. (1973). *Acta Cryst.* B**29**, 2006–2009.
FERRARIS, G. & FRANCHINI-ANGELA, M. (1972). *Acta Cryst.* B**28**, 3572–3583.
GIBBS, G. V., HAMIL, M. M., LOUISNATHAN, S. J., BARTELL, L. S. & YOW, H. (1972). *Am. Mineral.* **57**, 1578–1613.
ICHIKAWA, M. (1978). *Acta Cryst.* B**34**, 2074–2080.
ICHIKAWA, M. (1979). *Acta Cryst.* B**35**, 1300–1301.
PYATENKO, YU. A. (1973). *Sov. Phys. Crystallogr.* **17**, 677–682.
SHANNON, R. D. & CALVO, C. (1973). *J. Solid State Chem.* **6**, 538–549.
SHANNON, R. D. & PREWITT, C. T. (1969). *Acta Cryst.* B**25**, 925–946.

Acta Cryst. (1984). B**40**, 6–13

The Crystal Structures of Sodalite-Group Minerals

BY I. HASSAN* AND H. D. GRUNDY

Department of Geology, McMaster University, Hamilton, Ontario, Canada L8S 4M1

(*Received* 7 *April* 1983; *accepted* 1 *September* 1983)

Abstract

Sodalite, $Na_8(Al_6Si_6O_{24})Cl_2$, is cubic, $P\bar{4}3n$, $M_r = 969{\cdot}2$, $F(000) = 476$, $a = 8{\cdot}882(1)$ Å, $D_x = 2{\cdot}30$ Mg m^{-3}, $Z = 1$, $R = 0{\cdot}017$ for 157 unique observed reflections measured on an automated four-circle X-ray diffractometer using Mo $K\alpha$ radiation. The 1:1 aluminosilicate framework is completely ordered. A geometrical sodalite model has been developed, which, when calibrated with the parameters from the refined structure, enables: (1) the accurate prediction of the atomic coordinates of all members of the sodalite-group minerals at both room and elevated temperatures; (2) the prediction of the chemical limits of structural stability of all such materials; (3) thermal-expansion data and substitution of interframework ions to be rationalized and predicted in terms of the rotation of the (Al, Si)O_4 tetrahedra.

Introduction

Minerals in the aluminosilicate sodalite group are characterized by an ordered framework of AlO_4 and SiO_4 tetrahedra. The cubic symmetry is the result of the close packing of interconnected sixfold rings of (Al, Si)O_4 tetrahedra. These six-membered rings are stacked parallel to {111} in an *ABCABC*... type of sequence. The structure is further characterized by (Al, Si)O_4 rings of four tetrahedra parallel to {100}. The overall linkage of (Al, Si)O_4 tetrahedra results in a cubo-octahedral cavity (Fig. 1). The six-membered rings form continuous channels that offer diffusion paths for interframework ions (Barrer & Vaughan, 1971).

The aluminosilicate framework of the sodalite-group minerals $(Al_6Si_6O_{24})^{6-}$ is isotypic with the framework of beryllosilicate $(Be_6Si_6O_{24})^{12-}$ (Pauling, 1930); borate $(B_{12}O_{24})^{12-}$ (Smith, García-Blanco & Rivoir, 1961); aluminate $(Al_{12}O_{24})^{12-}$ (see Depmeier, 1979); and the naturally occurring mineral tugtupite ($Na_8Al_2Be_2Si_8O_{24}Cl_2$) (Danø, 1966). Ga- and Ge-substituted analogues of the aluminosilicate sodalites are also known (McLaughlan & Marshall, 1970). The sodalite cage is also used as a building unit in many zeolites (Meier, 1968) and several complicated structures, such as α-Mn, Sb_2Tl_7, tetrahedrite, *etc.*, can be described and related to that of sodalite (Nyman & Hyde, 1981). Within the sodalite cage a variety of cations and anions can be substituted. This paper examines in detail the aluminosilicate sodalites with interframework cations of the álkali group (Li^+, Na^+, K^+, Rb^+, Cs^+) and anions of the halide group (F^-, Cl^-, Br^-, I^-), and also the naturally occurring sulphatic sodalites nosean and hauyne.

Many of these sodalites have been synthesized by Henderson & Taylor (1977) and a computer model

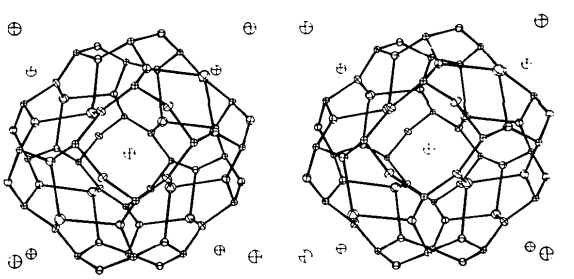

Fig. 1. Stereoscopic view of the sodalite structure showing the arrangement of AlO_4 and SiO_4 tetrahedra which gives the cubo-octahedral cavity. Small thermal ellipsoids represent Al or Si atoms, intermediate the framework oxygen, large the Na atoms in the vicinity of the six-membered rings and the isolated Cl atoms at the corners and centre of the cell.

* Present address: Earth and Planetary Sciences, Erindale Campus, University of Toronto, Ontario, Canada L5L 1C6.

0108-7681/84/010006-08$01.50

for the crystal structure of sodalite was developed by Taylor & Henderson (1978). This model was later replaced by the distance least squares (DLS) modelling technique of Dempsey & Taylor (1980) and still more recently by a new computer model of Beagley, Henderson & Taylor (1982).

A geometrical model for sodalite has been developed in this paper and, to provide the necessary parameters for structural calculations, an accurate X-ray single-crystal structure refinement of sodalite (proper) was undertaken. This geometrical model can also be used to re-analyse thermal expansion data reported by Taylor (1968, 1972) and Henderson & Taylor (1978) for aluminosilicate sodalites. They observed increasing rate of expansion up to the highest temperature studied, except for the SO_4^{2-} and I^--bearing aluminosilicate sodalites which exhibited a sharp change in rate giving rise to a discontinuity. The expansion is due to the untwisting of the partially collapsed framework by rotation of the $(Al, Si)O_4$ tetrahedra. The driving force for the untwisting can arise either by expansion of the bonds of the cavity ions (Henderson & Taylor, 1978) or in the framework itself with the bonds of the cavity ions acting as a restraint (Dempsey & Taylor, 1980). Discontinuities are thought to occur either when the fully-expanded state is achieved (Taylor, 1968, 1972) or when the cation is at 1/4 (Henderson & Taylor, 1978; Dempsey & Taylor, 1980).

The sodalite model

In sodalite (proper) the framework is in a partially collapsed state owing to rotation of the $(Al, Si)O_4$ tetrahedra so that the Na atom is within reasonable bonding distance to both the framework oxygens and the Cl atom on the 2(*a*) site. This collapse of the framework reduces the cell edge from 9·4Å for the expanded framework to 8·8 Å (Pauling, 1930).

The geometry of this collapse can be evaluated by considering a fully-expanded framework of perfectly regular tetrahedra of equal sizes sharing corners (Fig. 2*a*). Without a change in topology, the geometry of this array of tetrahedra can be changed by rotating each tetrahedron about directions which are parallel to the cell edges (*i.e.* their $\bar{4}$ axes). The relationship between the cell edge, *a*, the edge of the tetrahedra, *E*, and the angle of rotation, φ, is (Taylor, 1972)

$$a = E(2\cos\varphi + \sqrt{2}) \tag{1}$$

and the coordinates of the corner (x, x, z) of the tetrahedra are (Nyman & Hyde, 1981)

$$x = \frac{\cos\varphi}{2(2\cos\varphi + \sqrt{2})}$$
$$z = \frac{\sin\varphi}{2(2\cos\varphi + \sqrt{2})}, \tag{2}$$

where

$$\varphi = \tan^{-1}(z/x). \tag{3}$$

When the tetrahedra are rotated, the space group is changed from $Im3m$ to $I\bar{4}3m$. However, in sodalite, the observed symmetry is $P\bar{4}3n$. This is due to the ordering of the Al and Si and results in AlO_4 and SiO_4 tetrahedra of unequal size that are compressed slightly along their rotation axes (Pauling, 1930) and also two rotation angles φ_{Si} and φ_{Al} that correspond to the rotation of the SiO_4 and AlO_4 tetrahedra, respectively (Fig. 2).

The geometry of the sodalite framework can be determined if two assumptions are made: (i) that the Al–O and Si–O distances are constant irrespective of the interframework ions; (ii) that the two O–O edges, E_{Al} and E_{Si} (Fig. 2), of the AlO_4 and SiO_4 tetrahedra, respectively, are also constant. Comparison of the structures of sodalite (proper) (this work) and basic sodalite, $Na_8(Al_6Si_6O_{24})(OH)_2.2H_2O$ (Hassan & Grundy, 1983) shows that the interframework anions have no effect on these distances. Moreover, the refinements of six members of the helivite group of minerals, $(Mn, Zn, Fe)_8(Be_6Si_6O_{24})S_2$, covering the entire compositional series (Hassan & Grundy, 1984) show that different interframework cations also have no effect on similar tetrahedral distances. The bond-valence calculations of Brown & Shannon (1973) would also support these assumptions since bond distance is a fundamental concept in their model. Using these assumptions and a measured cell edge the entire geometry of the aluminosilicate framework can be calculated.

The cell edge, *a*, can be obtained from the geometry of the array of tetrahedra shown in Fig. 2(*b*). Those tetrahedra which show a square outline in projection have E_{Al} or E_{Si} as their body diagonals and are rotated about a direction parallel to a_3 by $\varphi_{Al}°$ or $\varphi_{Si}°$, respectively. For all other tetrahedra E_{Al} or E_{Si} is normal to the a_1 or a_2 edges and their corresponding rotations are about these directions. Therefore, the cell edge is given by

$$a = 2E_{Si}\cos\varphi_{Si} + 4[(Al\text{–}O)^2 - (E_{Al}/2)^2]^{1/2}, \tag{4}$$

where, by transformation,

$$\cos\varphi_{Si} = \frac{1}{2E_{Si}}\{a - 4[(Al\text{–}O)^2 - (E_{Al}/2)^2]^{1/2}\}. \tag{5}$$

These equations are symmetrical with respect to Al and Si and they give the variation of φ_{Si} and φ_{Al} with cell edge. The relationship between the Si–O–Al angle and the cell edge is obtained from the triangle $Al(\frac{1}{4}, 0, \frac{1}{2})$–$O(x, y, z)$–$Si(0, \frac{1}{4}, \frac{1}{2})$ and is

$$\cos(Al\text{–}O\text{–}Si) = \frac{Si\text{–}O}{2(Al\text{–}O)} + \frac{Al\text{–}O}{2(Si\text{–}O)} - \frac{a^2}{16(Si\text{–}O)(Al\text{–}O)}. \tag{6}$$

The atomic coordinates of the oxygen at the top left (O_{44}) in Fig. 2(*b*) are obtained from the two tetrahedra that it shares. The coordinates are

$$\begin{aligned} x &= \frac{1}{a}(E_{Si}/2)\cos\varphi_{Si} \\ y &= \frac{1}{a}(E_{Al}/2)\cos\varphi_{Al} \\ z_{Si} &= \frac{1}{2}-\frac{1}{a}(E_{Si}/2)\sin\varphi_{Si} \\ z_{Al} &= \frac{1}{2}-\frac{1}{a}(E_{Al}/2)\sin\varphi_{Al}, \end{aligned} \tag{7}$$

where

$$z = \tfrac{1}{2}(z_{Al}+z_{Si}),$$

so that

$$\begin{aligned} \varphi_{Si} &= \tan^{-1}[(\tfrac{1}{2}-z)/x] \\ \varphi_{Al} &= \tan^{-1}[(\tfrac{1}{2}-z)/y]. \end{aligned} \tag{8}$$

The z coordinate obtained from either the AlO_4 or SiO_4 tetrahedra should be equal but to avoid bias in calculations the mean value is used.

Calibration of the sodalite model

(i) *Refinement of the structure of sodalite (proper)*

Sodalite (proper) from Princess Mine, Bancroft, Ontario, equidimensional fragment, 0·22 mm, chemical analysis (X-ray fluorescence) (wt %) SiO_2 36·55, Al_2O_3 31·78, Na_2O 25·30, CaO 0·25, Fe_2O_3 0·19, K_2O 0·10, MnO 0·01, MgO 0·19, Cl 7·17, S 0·02, total 101·56 less O = Cl,S 1·62, net 99·94, calculated cell contents (based on Al + Si = 12), Si 5·93, Al 6·07, Na 7·95, Ca 0·04, Fe 0·02, K 0·02, Mn 0·00, Mg 0·05, Cl 1·97, S 0·01; precession photographs show sharp reflections and no superstructure, symmetry consistent with accepted space group $P\bar{4}3n$ (Löns & Schulz, 1967), cell parameter determined by least squares, 15 reflections, automatic four-circle single-crystal diffractometer, all reflections (1558) in the octant with h,k and l positive ($0 \le h, k, l \le 13$) out to a maximum 2θ of 65°. Nicolet $P3$ four-circle diffractometer, θ–2θ scan mode, 2θ scan range ($K\alpha_1 - 0{\cdot}85°$) to ($K\alpha_2 + 0{\cdot}85°$), variable scan rates of 3 to 29·3° min^{-1} dependent on the intensity of a prescan; two standard reflections, 211 and 222, monitored after every 50 reflections did not change; Lorentz, polarization and background effects and spherical absorption (μR = 0·21) corrections, equivalent reflections averaged to produce 309 unique reflections, 157 considered observed on the criterion $F_o > 3\sigma(F)$; all crystallographic calculations were made using XRAY76 (Stewart, 1976).

Initial positional parameters were those of Löns & Schulz (1967). Atomic scattering factors for neutral atoms were taken from Cromer & Mann (1968). The full-matrix least-squares refinement on $|F|$, using unit weights, converged to $R = \sum(|F_o| - |F_c|)/\sum|F_o| =$ 0·017 and $R_{(\omega=1)} = [\sum\omega(|F_o| - |F_c|)^2/\sum\omega|F_o|^2]^{1/2} =$ 0·021 for the 157 observed reflections.*

* List of structure factors, anisotropic thermal parameters and Tables 3, 4 and 5 have been deposited with the British Library Lending Division as Supplementary Publication No. SUP 38823 (5 pp.). Copies may be obtained through the Executive Secretary, International Union of Crystallography, 5 Abbey Square, Chester CH1 2HU, England.

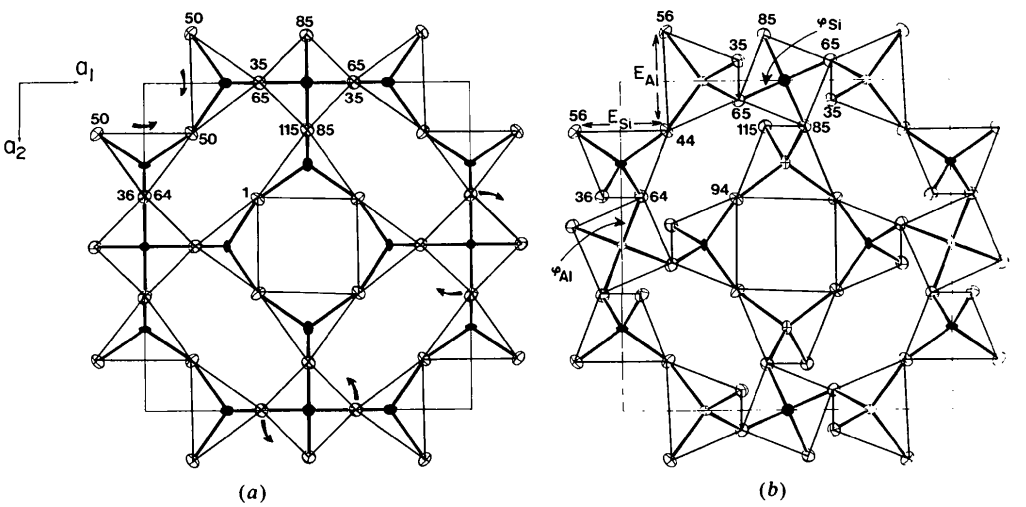

(*a*) (*b*)

Fig. 2. Upper half of unit cell. (*a*) The fully expanded framework of regular tetrahedra of equal sizes (space group $Im3m$). Arrows indicate the rotation of tetrahedra about axes parallel to the cell edges which collapse the framework. Along each row of tetrahedra orientated with their $\bar{4}$ axes parallel to a cell edge, alternate tetrahedra are rotated clockwise and anti-clockwise. (*b*) The partially collapsed structure of sodalite showing rotation angles φ_{Al} and φ_{Si} and also O–O distances E_{Al} and E_{Si}. The Al and O atoms are shown as open and the Si atoms as filled ellipsoids. Numbers indicate heights in units of one-hundredth on the projection axis, a_3.

Table 1. *Atomic positional parameters and thermal parameters* ($Å^2 \times 10^4$), $U_{eq} = 1/3$ *trace* $\tilde{U}$

	Occupancy	Site	x	y	z	U_{eq}
Na	1·0	8(*e*)	0·1778 (2)	0·1778	0·1778	198
Cl	1·0	2(*a*)	0	0	0	249
Si	1·0	6(*c*)	$\frac{1}{4}$	$\frac{1}{2}$	0	79
Al	1·0	6(*d*)	$\frac{1}{4}$	0	$\frac{1}{2}$	81
O	1·0	24(*i*)	0·1390 (3)	0·1494 (3)	0·4383 (2)	122

Table 2. *Selected bond distances* (Å), *angles* (°) *and valence sums* (*valence units*), *e.s.d.'s in parentheses*

Si–O	4×1·620 (2)	Al–O	4×1·742 (2)
O–O	4×2·616 (3)	O–O	4×2·831 (3)
	2×2·701 (3)		2×2·871 (3)
Mean	2·644	Mean	2·844
O–Si–O	4×107·7 (1)°	O–Al–O	4×108·7°
	2×113·0 (1)		2×111·0
Mean	109·5	Mean	109·5
Si–O–Al	138·2 (1)°	Sodium coordination	
φ_{Si}	23·9	Na–Cl	2·736 (1)
φ_{Al}	22·4	Na–O	3×2·353 (2)
			3×3·087 (2)

Bond-valence sums
Si = 4×1·005 (5) = 4·021 (10)
Al = 4×0·736 (3) = 2·945 (7)
Na = 0·25 + 3×0·2080 (1) + 3×0·0450 (1) = 1·009 (1)
O = 1·005 (5) + 0·736 (3) + 0·208 (1) + 0·045 (1) = 1·994 (10)

of the populations of the Na and Cl sites shows both to be fully occupied and consistent with the chemical analysis. The refinement was repeated with all 309 reflections treated as observed which gave $R = 0·039$ and $R_{(\omega=1)} = 0·036$ with no significant change in parameters. The final parameters are given in Table 1.

(ii) *Discussion of the structure of sodalite* (*proper*)

Interatomic distances, angles and bond-valence sums (Brown & Shannon, 1973) about the atoms are given in Table 2. The Al and Si ions are charge balanced and therefore the Al–O and Si–O distances are indicative of complete ordering of the framework.

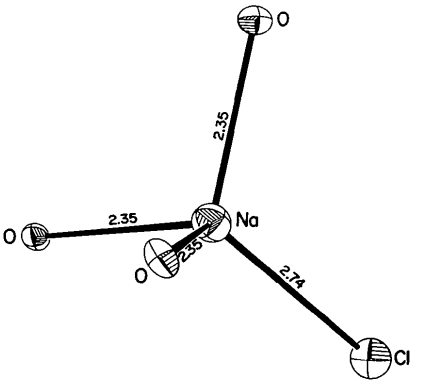

Fig. 3. Fourfold coordination of the Na site in sodalite. Na–O and Na–Cl distances (Å) are referred to as C–O and C–A, respectively (see text).

Each of the eight six-membered rings has one sodium neighbour and the ring is strongly distorted such that three of the oxygen atoms are at a distance of 2·353 (2) Å and three at 3·087(2)Å to the sodium atom. This distortion is a result of the displacement of Na by 1·11(1)Å from the mean plane of the ring due to the Na–Cl bond. The sodium is therefore closely coordinated by only three oxygens and one chlorine arranged as a trigonal pyramid (Fig. 3). Chlorine is tetrahedrally coordinated by sodium.

(iii) *Derived equations*

Substituting the calculated distances (Al–O = 1·7417 Å, Si–O = 1·6195 Å, $E_{Al} = 2·8710$ Å and $E_{Si} = 2·7010$ Å) obtained from the refined atomic coordinates in (4), (5) and (7) give, respectively,

$$a = 5·7420 \cos \varphi_{Al} + 3·5753 = 5·4020 \cos \varphi_{Si} + 3·9453, \quad (4')$$

$$\cos \varphi_{Si} = a/5·4020 - 0·7303 \qquad \cos \varphi_{Al} = a/5·7420 - 0·6227 \quad (5')$$

and

$$x = \tfrac{1}{4} - 0·9863/a, \qquad y = \tfrac{1}{4} - 0·8938/a$$
$$z_{Si} = \tfrac{1}{2} - 1·3505 (\sin \varphi_{Si}/a) \qquad z_{Al} = \tfrac{1}{2} - 1·4355 (\sin \varphi_{Al}/a). \quad (7')$$

We can therefore calculate the aluminosilicate framework parameters if the cell edge is known by using (5′) and (7′).

The structure is completed by fixing either the interframework-cation–framework-oxygen (C–O) distance or the interframework-cation–anion (C–A) distance (Fig. 3). We have chosen to fix the C–O distance since it can usually be predicted with greater accuracy.

In the above derivations, the cell edge for a particular sodalite must be known. However, we can calculate the cell edge (hence the structure) for any sodalite by estimating both the C–O and C–A distances and then using formulae which relate these distances to the atomic coordinates: $C(X, X, X)$, $O(x, y, z)$ and $A(0, 0, 0)$. The formulae are as follows:

$$X^2 - \frac{2}{3}(x+y+z)X + \frac{1}{3}\left[(x^2+y^2+z^2) - \left(\frac{C-O}{a}\right)^2\right] = 0 \quad (9)$$

and

$$X = \frac{C-A}{\sqrt{3}\,a}, \quad (10)$$

from which the cell edge, a, is obtained (see Fig. 6). If the cell edge is known these equations provide an independent check on the validity of the C–O, C–A estimates.

Results

(i) *Calculated structures for alkali-halide aluminosilicate sodalites*

We can approximate C–O and C–A distances by the sum of their atomic radii. Thus, if the radius of Na^+ (r_{NA^+}) is 0·990 Å, then from the refined structure of sodalite $r_{O^{2-}} = 1{\cdot}363$ Å and $r_{Cl^-} = 1{\cdot}746$ Å. These radii and others from Shannon (1976) are used.

The sodalite species is represented as follows: end member $Na_8(Al_6Si_6O_{24})Cl_2$ by Na_8Cl_2-sodalite and solid-solution $Na_4K_4(Al_6Si_6O_{24})Cl_2$ by $Na_4K_4Cl_2$-sodalite, *etc.* Among the sodalites synthesized and cell parameters determined at various temperatures by Henderson & Taylor (1978) the following seven species are selected for detailed study: (1) Li_8Cl_2-; (2) $Li_{4\cdot4}Na_{3\cdot6}Cl_2$-; (3) Na_8Cl_2-; (4) Na_8Br_2-; (5) Na_8I_2-; (6) $Na_4K_4Cl_2$- and (7) $Na_{0\cdot4}K_{7\cdot6}Cl_2$-sodalite. Their calculated structures at room temperature are presented in Table 3.*

For Li_8Cl_2-sodalite, the radii sum gave Li–O = 1·953 Å. This distance gave a Li–Cl distance of 2·819 Å which is much larger than the distance of 2·565 Å in lithium chloride. This was also reported by Taylor & Henderson (1978) and Dempsey & Taylor (1980). To correct this anomaly and to make calculated Li–halide distances at least comparable to those obtained from the sum of atomic radii, a Li–O distance of 2·102 Å is used in the calculations.

Table 4* consists of calculated structures of Li_8F_2-, Li_8Br_2-, Li_8I_2-, Na_8F_2-, K_8F_2-, $Na_{0\cdot5}K_{7\cdot5}Br_2$- and Rb_8F_2-sodalite that are predicted to exist but have not yet been synthesized. The calculations show that, with the exception of Rb_8F_2-sodalite, Rb-halide and Cs-halide sodalites are not structurally stable owing to the large size of the Rb and Cs cations.

The room-temperature atomic parameters for the aluminosilicate sodalites are different from those calculated by Taylor & Henderson (1978) and Dempsey & Taylor (1980). Beagley, Henderson & Taylor (1982) have used X-ray powder data to refine the structures of Na_8Cl_2-, Li_8Cl_2-, $K_{7\cdot6}Na_{0\cdot4}Cl_2$-sodalites in the space group $P\bar{4}3n$ and Na_8I_2-sodalite in the space group $I\bar{4}3m$. The calculated information for these structures using the improved computer model of Beagley, Henderson & Taylor (1982) and the geometrical model agree to within 0·003 in atomic coordinates when using space group $P\bar{4}3n$. This discrepancy can be traced to the use of the sodalite (proper) cell edge of Löns & Schulz (1967) in the calibration of the computer model and which now appears to be too small. However, the maximum difference between both models and the refined structures increases to 0·005 in atomic coordinates and probably reflects the difficulty of obtaining accurate structural parameters from powder data. In the case of Na_8I_2-sodalite the refinement was made with space group $I\bar{4}3m$ although Beagley, Henderson & Taylor (1982) were doubtful that the implied Al–Si disorder was in fact present. The model calculations would suggest that $P\bar{4}3n$ is the preferred space group; also, structural refinements of other sodalites with a 1:1 ratio of Al:Si and similar interframework ions show complete Si–Al ordering within their frameworks. These include basic sodalite (Hassan & Grundy, 1983), sodalite (this work), nosean (Hassan & Grundy, 1984*a*) and hauyne (Hassan & Grundy, 1984*b*).

Therefore, the computer model of Beagley, Henderson & Taylor (1982) and our geometrical model give essentially the same results; however, they are different in many respects although both models require fixed Al–O and Si–O distances. The computer model must have an experimental cell edge; while our model normally uses such a parameter, it is not essential. To determine the framework geometry, the computer model solves three non-linear simultaneous equations incorporating a weighted mean of the oxygen x and y coordinates while the geometrical model requires two O–O distances, one from each distinct framework tetrahedron. To complete the structure, the computer model requires an estimated C–A distance while the geometrical model generally uses an estimated C–O distance. As the single-crystal structure determinations of sodalite-type minerals confirms the relative consistency of the O–O distances, the geometrical model is easier to control and consequently has a more general application than the computer model of Beagley, Henderson & Taylor (1982). They estimate C–A distances by combining the method of Beagley (1975) and Brown & Shannon (1973), and state that C–O distances estimated from atomic radii are unreliable. In the case of the Li-sodalites this is indeed the case and is obviously due to the highly polarizing nature of the Li^+ ion. However, for other aluminosilicate sodalites, C–O distances estimated from atomic radii (Shannon, 1976) are consistent with the structural refinements and the model results of Beagley, Henderson & Taylor (1982). The use of C–O distances rather than C–A distances is essential to the rationalization of the thermal expansion of sodalitic materials. In the case of Li-sodalites a useful Li–O distance can be calculated by using the geometrical model and a measured value for the cell edge of Li_8Cl_2-sodalite and an estimated Li–Cl distance using atomic radii of Shannon (1976).

(ii) *Maximum and minimum cell edges*

The maximum cell edge is obtained when $\varphi_{Al} = 0$ since the AlO_4 tetrahedron reaches this critical point before the SiO_4 tetrahedron. Therefore, $a_{max} =$ 9·317 Å (equation 4′). A structure calculated using

* See deposition footnote.

this cell edge and a hypothetical cation at 1/4 is given in Table 4.* The minimum cell edge should correspond to the Li_8F_2-sodalite for which $a_{min} = 8{\cdot}141$ Å (Table 4) since these are the smallest ions. The average change in rotation of the tetrahedra from the minimum to the maximum cell edge is 33°, with an increase in the Si–O–Al angle of 40° and in the Al–Si distance of 0·416 Å.

(iii) *Sulphatic sodalites (nosean and hauyne)*

The geometrical model can be used to show which species have peculiarities. In this regard, nosean, ideally $Na_8(Al_6Si_6O_{24})SO_4$, and hauyne, ideally $Na_6Ca_2(Al_6Si_6O_{24})(SO_4)_2$, can be shown to be interesting materials. The structures calculated from the geometrical model are given in Table 5.*

There are two equally probable 8(*e*) cation sites [*C*(1) and *C*(2)] located on the body diagonal of the cubic cell that have identical distances to the oxygens of a particular six-membered ring of framework tetrahedra and likewise two possible 8(*e*) sites on the same body diagonal for the oxygen of the SO_4 group [O(1) and O(2)]. Let us assume that the oxygens of the SO_4 group lie on the O(1) site, then the *C*(1)–O(1) distance is too short to be a bond distance and thus the *C*(2) site is occupied with the *C*(1) vacant. Similarly, if the O(2) site is occupied then *C*(2) must be vacant. Since *C*(1) and *C*(2) sites are in close proximity, only one can be occupied at any one time, which restricts the location of the SO_4 group.

Also possible is the case in which the cation sites form bonds with the three oxygens of the base of the SO_4 tetrahedron; however, this seems less attractive an option owing to the short cation–sulphur distance.

The structures of nosean and hauyne have been determined and preliminary evaluation of these seems to bear out the foregoing predictions.

(iv) *Thermal expansion of the sodalites*

The thermal expansion of the seven selected sodalite species are replotted in Fig. 4. Among the alkali-halide aluminosilicate sodalites, a discontinuity was recognized only for Na_8I_2-sodalite by Henderson & Taylor (1978).

The thermal-expansion behaviour of aluminosilicate sodalites can be studied by calculating structures at elevated temperatures. In the absence of structural data at such temperatures, we may assume that changes in the tetrahedral dimensions are slight and may be neglected to a first approximation without loss in generality. This approximation may be an excellent one since the framework tetrahedra have considerable rotational freedom. To complete the sodalite structure we need to predict the *C*–O and/or *C*–*A* bond at elevated temperatures.

The characteristics of the *C*–O bond can be examined after the cation has reached 1/4 since it is not necessary to make any assumptions regarding *C*–O and *C*–*A* distances. After such calculations are made, the *C*–O distances can be extrapolated to temperatures where the cation is less than 1/4. The Na_8I_2-sodalite is ideal for such an analysis.

The variation of the Na–O distance with temperature is shown in Fig. 5(*a*). It can be seen that the expansion of the Na–O bond is quite small when the cation is $\leq 1/4$. The *C*–O distances in general can therefore be considered constant and equal to the room-temperature distance up to where the cation is $\leq 1/4$. This contrasts with the assumption made by Dempsey & Taylor (1980).

Based on the above, structures were calculated (Hassan, 1982) at each temperature up to the highest temperature studied by Henderson & Taylor (1978). However, results only for room- and the highest temperature are given in Table 3. For the Na_8I_2- and Na_8Br_2-sodalites, results for a few intermediate temperatures are also included. All the results, however, are shown graphically in Fig. 5.

The discontinuity for Na_8I_2-sodalite was recognized at $T = 1083$ K, $a = 9{\cdot}168$ Å, by Henderson & Taylor (1978). Based on the replotted data and structural calculations, the discontinuity is predicted to occur at $T = 1023$ K, $a = 9{\cdot}155$ Å. The cell edge for Na_8Br_2-sodalite at 1333 K was considered to be unreliable. Even if we ignore this data point and use the data at 1273 K, calculations (Table 3) show that a discontinuity is just about to be reached. In fact, the discontinuity is predicted to occur at $T = 1283$ K,

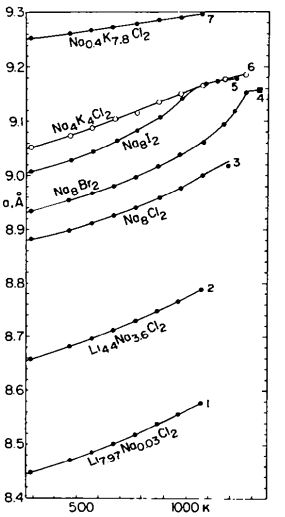

Fig. 4. Thermal expansion of cell edge (*a*) for seven aluminosilicate sodalites selected and replotted from the data of Henderson & Taylor (1978) and identified by their complement of inter-framework atoms.

* See deposition footnote.

$a = 9{\cdot}155$ Å, indicating that the data point at 1333 K is valid.

Discontinuities for Na_8I_2- and Na_8Br_2-sodalites, seen in Fig. 4 when $a = 9{\cdot}155$ Å (see Fig. 6), are due to the cations reaching 1/4 (Fig. 5*a*) and, as a result, discontinuities occur in the C–A distances (Fig. 5*b*).

Equation (9) can be used to show the variation of the cation coordinate with cell edge for constant C–O distances. [Note: intersection of these curves with (10) gives unknown cell edges.] Fig. 6 shows curves for various constant C–O distances.

A boundary separates the alkali-halide sodalites into two groups. This boundary corresponds to a C–O curve that passes through the point (a_{max}, $X = 1/4$) and occurs just to the right of the curve that describes the $Na_4K_4Cl_2$-sodalite. All the sodalites that lie to the left of this boundary follow C–O curves until the cation is at 1/4. In particular, the Na-halide sodalites should follow the Na–O = 2·353 Å curve to a cell edge of 9·155 Å where the Na^+ ion is at 1/4. Similarly, the Li-halide sodalites should show a discontinuity at $a = 8{\cdot}835$ Å. Whether a discontinuity occurs in practice depends on the thermal stability of the sodalite in question. Based on thermal-expansion data and on the degree of collapse, the Li-halide and Na_8F_2-sodalites are not expected to reach the discontinuity since sodalite (proper) decomposes before the discontinuity point.

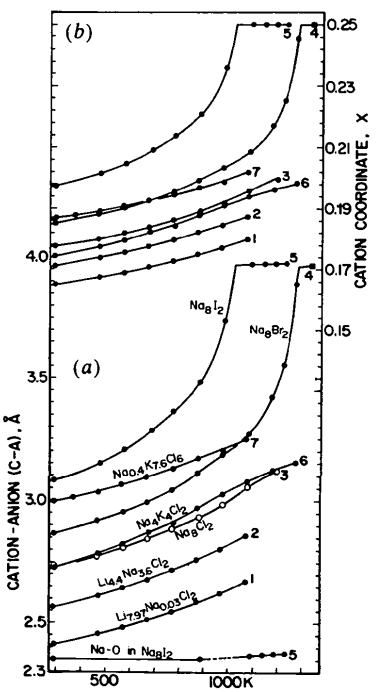

Fig. 5. (*a*) Variation of the interframework-cation–anion (C–A) distance with temperature. The variation of the Na–O distance in $Na_8(Al_6Si_6O_{24})I_2$ with temperature is also shown. (*b*) Variation of the interframework-cation fractional coordinate, X, with temperature.

The sodalites that lie to the right of the boundary have a different thermal-expansion behaviour. They first expand in the usual manner but instead of the cation reaching 1/4, the maximum cell edge is reached. One may also expect a sharp discontinuity at this point. However, the framework tetrahedra can distort together with the normal expansion of the C–A and C–O bonds. These changes will be very subtle and change in the thermal-expansion rate may be undetectable. The AlO_4 and SiO_4 tetrahedra are expected to distort in such a way as to make them more regular (and perhaps towards equal dimensions) since this leads to a theoretically larger maximum cell edge [equation (1): $a = 9{\cdot}365$ Å].

In this regard we note that the cell edge for $Na_{0\cdot3}K_{2\cdot9}Rb_{4\cdot8}(Al_6Si_6O_{24})Cl_2$ at room temperature is 9·316 Å, which is close to the maximum cell edge of 9·317 Å for a fully expanded framework in space group $P\bar{4}3n$. On heating to 973 K the cell edge is 9·336 Å. The mean thermal expansion of this sodalite is the least of all the sodalites studied by Henderson & Taylor (1978). This means that the increase in cell edge is the result of distortion of the framework tetrahedra. It is possible that, for this particular sodalite, the Al/Si framework is disordered, in which case the model with space group $I\bar{4}3m$ is perhaps more appropriate.

The difference in behaviour between the two groups of sodalites is clearly due to the size of the interframework cations. Li^+ and Na^+ ions are small

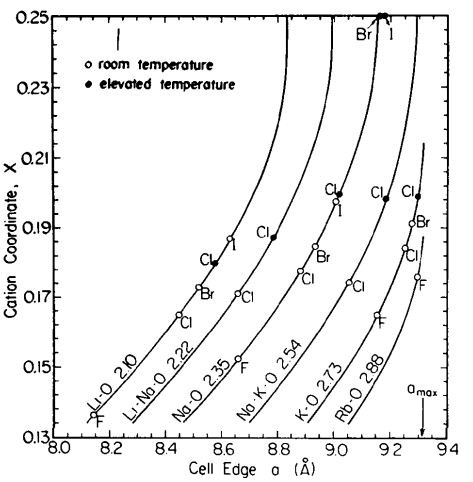

Fig. 6. Calculated variation of the interframework-cation fractional coordinate, X, with cell edge for constant interframework-cation–framework-oxygen (C–O) distances (equation 9). Intersection of the C–O curves with the interframework-cation–anion (C–A) curve (equation 10) gives the position of that sodalite and is represented by the halide ion. The full circles correspond to the highest temperature and the open circles to the room-temperature sodalites. The experimental cell edges and temperatures of Henderson & Taylor (1978) together with predicted cell edges from Table 4 and the geometrical model were used in the construction of the diagram which shows the entire compositional field of the aluminosilicate sodalites.

enough to enter the plane of the six-membered rings and form reasonable C–O distances and therefore these ions have the potential of producing a discontinuity, whereas K^+ and Rb^+ ions are too large to enter the rings and on expansion the maximum cell edge is reached. Substitution of various sizes of cations and anions has the same geometrical effect on the framework as heating.

Consequently, the driving force for the untwisting of the framework tetrahedra by heating (or substitution) must lie in the bonds of the cavity ions rather than in the framework itself. Therefore, the thermal expansion of sodalites is controlled by the expansion of the C–A bond (Fig. 3) which forces the cation towards 1/4, which in turn causes the framework tetrahedra to rotate. This gives rise to a high rate of expansion. When the cation is at 1/4 it is midway between two anions and in the plane of the six-membered ring; the anion is now eightfold coordinated. The expansion rate therefore decreases. From this point onwards the C–O bond also begins to expand. Continued temperature elevation after reaching the maximum cell edge must force the geometries of the two originally distinct framework tetrahedra to become the same, perhaps due to disorder of the Al and Si atoms culminating in a change of space group from $P\bar{4}3n$ to $I\bar{4}3m$.

(v) *Mean expansion coefficients for sodalites*

The relationship between cell edges and mean expansion coefficients has been interpreted as being due to the different C–A bonds having broadly similar force constants and to the dependence of the cell edge on the cosine of the tilt angle (Dempsey & Taylor, 1980). Henderson & Taylor (1978) noted, however, that several Na/K solid solutions, in particular $Na_4K_4Cl_2$-sodalite, should have a mean expansion coefficient that lies mid-way between those of the Na_8Cl_2- and K_8Cl_2-sodalites, but instead it lies close to the Na_8Cl_2-sodalite.

This anomalous behaviour may be rationalized in the following way. For the $Na_4K_4Cl_2$-sodalite, the weighted mean of the (Na, K)–Cl bond is not only identical to that of the Na–Cl bond in sodalite (proper) at low temperatures but is close to it at all temperatures (Fig. 5*a*). Therefore, the thermal expansion of $Na_4K_4Cl_2$-sodalite is governed in the early stages by the Na–Cl bond-expansion characteristics with the K^+ ion playing a minor role. The mean thermal expansion coefficient and C–A bond expansion is thus similar to the Na_8Cl_2 end member. As the temperature is increased and the cations move towards 1/4, the K^+ ion plays an increasingly important role since it cannot enter the plane of the six-membered ring and still form reasonable K–O distances. This behaviour strongly suggests that the Na^+ and K^+ cations are ordered into separate cavities.

(vi) *Chemical boundaries for alkali-halide aluminosilicate sodalites*

The entire alkali-halide aluminosilicate-sodalite compositional field is shown in Fig. 6. In general, going upward in Fig. 6 one sees the effect of increasing size of the halide ion and going to the right the effect of increasing size of the alkali cation. Fig. 6 clearly shows the geometrical existence of the end-member alkali-halide sodalites except K_8I_2-, Rb_8Cl_2-, Rb_8Br_2-, Rb_8I_2- and Cs-halide sodalites. Complete sodalite solid solutions appear possible between the cations Li^+ and Na^+, Na^+ and K^+ and to some extent between K^+ and Rb^+. It seems also possible to have mixed-halide sodalites, for example $Na_8(Al_6Si_6O_{24})ClBr$. So far only sodalite solid solutions with respect to the interframework cations have been synthesized.

Finally, and most importantly, a treatment similar to that presented in this paper can be made for all the cubic isotypes of sodalite and can be used to preview selected species for detailed experimental studies.

HDG thanks the Natural Sciences and Engineering Research Council of Canada for grants to support this work.

References

BARRER, R. M. & VAUGHAN, D. E. W. (1971). *J. Phys. Chem. Solids*, **32**, 731–743.

BEAGLEY, B. (1975). *Chem. Soc. Rev.* **3**, 52–71.

BEAGLEY, B., HENDERSON, C. M. B. & TAYLOR, D. (1982). *Mineral. Mag.* **46**, 459–464.

BROWN, I. D. & SHANNON, R. D. (1973). *Acta Cryst.* A**29**, 266–282.

CROMER, D. T. & MANN, J. B. (1968). *Acta Cryst.* A**24**, 321–324.

DANØ, M. (1966). *Acta Cryst.* **20**, 812–816.

DEMPSEY, M. J. & TAYLOR, D. (1980). *Phys. Chem. Miner.* **6**, 197–208.

DEPMEIER, W. (1979). *J. Appl. Cryst.* **12**, 623–626.

HASSAN, I. (1982). *The Crystal Structure and Crystal Chemistry of Sodalite and Cancrinite Groups of Minerals.* PhD Thesis, McMaster Univ.

HASSAN, I. & GRUNDY, H. D. (1983). *Acta Cryst.* C**39**, 3–5.

HASSAN, I. & GRUNDY, H. D. (1984*a*). In preparation.

HASSAN, I. & GRUNDY, H. D. (1984*b*). In preparation.

HENDERSON, C. M. B. & TAYLOR, D. (1977). *Spectrochim. Acta Part A*, **33**, 283–290.

HENDERSON, C. M. B. & TAYLOR, D. (1978). *Phys. Chem. Miner.* **2**, 337–347.

LÖNS, J. & SCHULZ, H. (1967). *Acta Cryst.* **23**, 434–436.

MCLAUGHLAN, S. D. & MARSHALL, D. J. (1970). *Phys. Lett. A*, **32**, 343–344.

MEIER, W. M. (1968). *Zeolite Structures.* In *Molecular Sieves*, pp. 10–27. London: Society of Chemistry for Industry.

NYMAN, H. & HYDE, B. G. (1981). *Acta Cryst.* A**37**, 11–17.

PAULING, L. (1930). *Z. Kristallogr.* **74**, 213–225.

SHANNON, R. D. (1976). *Acta Cryst.* A**32**, 751–767.

SMITH, P., GARCÍA-BLANCO, S. & RIVOIR, L. (1961). *Z. Kristallogr.* **115**, 460–463.

STEWART, J. M. (1976). Editor, the XRAY system. Tech. Rep. TR-446. Univ. of Maryland, College Park, Maryland, USA.

TAYLOR, D. (1968). *Mineral. Mag.* **36**, 761–769.

TAYLOR, D. (1972). *Mineral. Mag.* **38**, 593–604.

TAYLOR, D. & HENDERSON, C. M. B. (1978). *Phys. Chem. Miner.* **2**, 325–336.